Noise Analysis of Ultra High Speed SiGe BiCMOS Track and Hold Amplifier for Fiber Optic Equalizer

Hailang Liang, Rob.J. Evans and Efstratios Skafidas *

Abstract— **Noise performance of the switched emitter follower (SEF) track and hold (TH) amplifier is analyzed. Simulations based on a commercial available 130 nm SiGe HBT process technology are implemented with the SpectreRF circuit simulator. It is shown that both the thermal noise and shot noise contribute to the TH amplifier (THA) at ultra high frequency. Simulations also locate the major noise contributor in the SEF THA. Approximate expressions for the output noise of the major noise contributor of the THA are derived and the numerical experiment of the output noise is presented.**

Keywords: Track and hold amplifier, BiCMOS switched emitter follower, ultra high speed, noise location and noise model

1 Introduction

The fiber optic equalizer is an important element for optic fiber data communication systems, Fig.1 that is taken from [1] illustrates a system block diagram of a fiber optic equalizer. The high-speed analog-to-digital converters(ADCs) is the heart of the optic equalizer[1]. The THA is a crucial building block in ADCs since it makes a great impact on the dynamic performance of ADCs. To achieve high speed operation, the open loop architecture switched emitter follower is chosen for THA[1]. Noise is one of the important factors that limit the dynamic range of THA. As a result, it reduces the achievable resolution of the circuit. Therefore it is necessary to minimize this effect in order to improve the circuit performance. Theoretical noise analysis and numerical examples for switched capacitor amplifier circuits are present in [2]. To the best of our knowledge, noise analysis in SiGe HBT SEF THA has not been reported in the literature.

In this paper, we analyze the noise of major noise contributor in the hold mode of THA with the SEF configuration. Simulation and analysis show that, at ultra high frequency, both the thermal noise and shot noise contribute to the output noise, the flicker noise can be ignored. Section 2 describes the noise in a SEF THA for

*National ICT Australia, Department of Electrical and Electronic Engineering, University of Melbourne, Parkville 3010, Melbourne, Australia Email: h.liang@ee.unimelb.edu.au
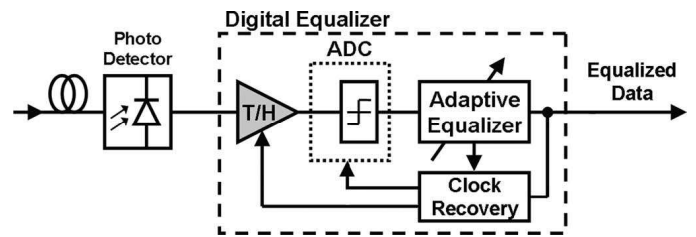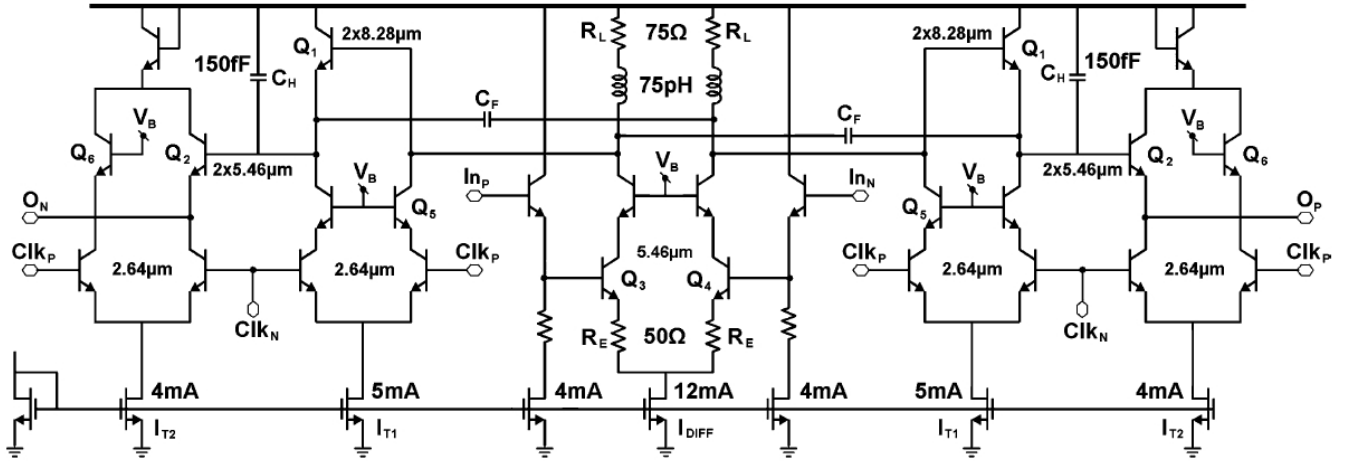
Figure 1: System block diagram of a fiber optic equalizer.

ultra high speed application. In section 3, noise model of bipolar junction transistor is presented. The major noise contributor in hold mode is given in section 4. Section 5 and section 6 show the numerical examples and the simulation results respectively and then follows by conclusion.

2 Noise in A SEF THA

Consider a SEF THA shown in Fig.5 in [1], which is a differential emitter follower THA illustrated in Fig.2. This common switched emitter follower architecture [1] [3] is suitable for ultra high speed application, it has a good isolation between the input and output signal in hold mode. However, the spurious-free dynamic range (SFDR) dynamic performance of this circuit is low, for instance, the maximum SFDR value shown in [1] is less than 39 dB with the input frequency from 1GHz to 19GHz, which indicates the effective number of bit (ENOB) of the circuit is less 6.5. This limits its application in high resolution (ENOB > 8) ultra high speed data processing. An effective approach to improve the dynamic performance of the SEF THA is decreasing the noise magnitude of the major noise contributor among the THA.

As shown in Fig.6 in section 6, performing the noise simulation on the SEF THA (Fig.5 of [1]) denotes that the noise contribution from hold mode is much larger than that from track mode. It also shows in Fig.7 that the major noise contributor in hold mode is the HBT Q_{21} (Q_2 in Fig.5 of [1]). Therefore It is crucial to investigate the noise behavior of the transistor Q_{21} in order to reduce the noise effects to the THA.

Figure 2: A SEF THA shown in Fig.5

3 Noise Model of Bipolar Junction Transistor

The derivation of noise parameter equations is based on a complete SiGe BiCMOS equivalent circuit model [4], where we lumped the resistive elements of the base, emitter and collector respectively. These lumped base resistance contribute noise to the transistor. Fig. 3 shows a complete noise equivalent circuit for the bipolar junction transistor, where r_b, r_c and r_e are the lumped resistance of the base, emitter and collector respectively. r_π is the dynamic emitter resistance, $r_\pi = \frac{\beta}{g_m}$, β is the small signal current gain of the transistor. r_μ is collector base resistance. C_π is the dynamic emitter capacitance, it contains the base-charging capacitance C_b and the emitter-base depletion layer capacitance C_{je}, $C_\pi = C_b + C_{je}$. C_μ is the collector base transition capacitance plus diffusion capacitance due to base width modulation. Note that r_0 does not contribute noise since it is not a physical resistor. $\overline{v_{rb}^2}$, $\overline{v_{rc}^2}$ and $\overline{v_{re}^2}$ are the thermal noise voltage power spectral densities due to the base, collector and emitter resistance respectively. $\overline{i_b^2}$ and $\overline{i_c^2}$ represent the base and collector shot noise current power spectral density respectively. In ultra high speed operation, The flicker noise of the base can be ignored. The shot noise power spectral densities of the base and collector can be denoted as equation (1) and equation (2) respectively.

$$\overline{i_b^2} = 2qI_B\Delta f \tag{1}$$

$$\overline{i_c^2} = 2qI_C\Delta f \tag{2}$$

The collector and base shot noise are partially correlated, the cross-power spectral density between the base and collector shot noise can be formulated as equation (3) [5].

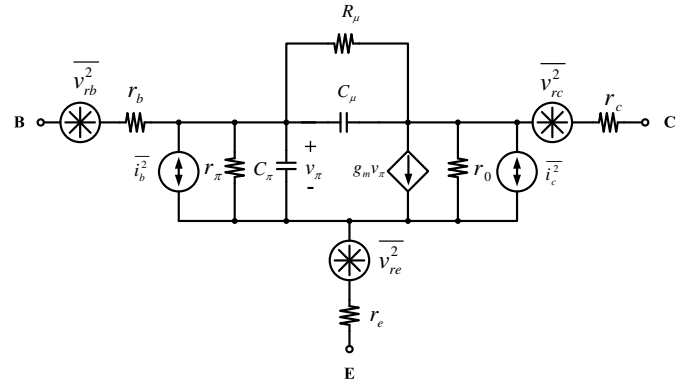$$< i_b^* i_c > = 2qI_C[\exp(-j\omega\tau_n) - 1]\Delta f, \tag{3}$$

Figure 3: Complete noise model of SiGe bipolar transistor

where q is the positive electron charge, Δf is the bandwidth in hertz over which the noise is measured. I_B and I_C are the DC base and collector currents respectively, ω is the angular frequency and τ_n is the noise transition time, which models the time delay between the base and collector shot noise currents. The correlation term $\exp(-j\omega\tau_n) - 1$ becomes significant when the frequency approaching f_T [6]. The noise power spectral densities for the resistances r_b, r_c and r_e are described as equation (4),equation (5) and equation (6) respectively.

$$\overline{v_{rb}^2} = 4K_BTr_b\Delta f, \tag{4}$$

$$\overline{v_{rc}^2} = 4K_BTr_c\Delta f, \tag{5}$$

$$\overline{v_{re}^2} = 4K_BTr_e\Delta f, \tag{6}$$

where K_B is the Boltzmann constant and T is the Kelvin absolute temperature. Unlike the shot noise, these thermal noise sources are assumed to be uncorrelated. We also assume $\overline{v_{rb}^2} = 4K_BTr_b\Delta f$ without introducing significant errors, since r_b is not completely a resistive compo-

4 Major Noise Contributor in Hold Mode

The major noise contributor in hold mode is Q_{21} (Q_2 in Fig.5 of [1]), The small signal equivalent circuit of Q_{21} is illustrated in Fig.4. In term of the complete noise mode shown in Fig.3, To figure out which noise source in Q_{21} contributes more noise, First,by applying KCL at the nodes A, B and C, the following equations (7), (8) and (9)are obtained respectively.

$$i_b + \frac{V_\pi}{r_\pi} + sC_\pi V_\pi + g_m V_\pi + \frac{(V_{XB} - V_{XA})}{r_0} + i_c - I_{OM} = 0 \quad (7)$$

$$-g_m V_\pi - \frac{(V_{XB} - V_{XA})}{r_0} - i_c + I_{CM} + sC_\mu(V_{XC} - V_{XB}) + \frac{V_{XC} - V_{XB}}{R_\mu} = 0 \quad (8)$$

$$-i_b - \frac{V_\pi}{r_\pi} - sC_\pi V_\pi - sC_\mu(V_{XC} - V_{XB}) - \frac{V_{XC} - V_{XB}}{R_\mu} + I_{BM} = 0 \quad (9)$$

It follows that four additional equations (10), (11), (12) and (13) are formulated by applying KVL.

$$V_\pi = V_{XC} - V_{XA} \quad (10)$$

$$V_A - V_{XC} = V_{rb} + I_{BM} r_b \quad (11)$$

$$V_{XA} - V_{out} = V_{re} + I_{OM} r_e \quad (12)$$

$$V_C - V_{XB} = V_{rc} + I_{CM} r_c \quad (13)$$

Solving these seven equations (7)-(13) yields the noise transfer function to the output, which is formulated in equation (14).

To simplify the analysis, H_1, H_2 and H_3 in equation (14) are neglected and thus yields the following equation (15).

Due to the three uncorrelated continuous-time noise sources V_{re}, V_{rb} and V_{ra}, and the two partial correlated noise source i_b and i_c, the spectral noise density at track mode output is formulated as equation (16). As shown in equation (16), there is little noise at low frequency but huge noise at ultra high frequency.

The total output noise is given by equation (17). It can be seen that the total noise depends on the thermal noise, shot noise ,parasitic capacitance and parasitic resistance. If we assume R_μ, r_e, r_b, r_π, r_0, g_m, q, I_B and I_C are constant, then α, β and γ is constant. Since

$$\omega_0 Q \propto \{C_\pi, C_\mu\},$$

$$\omega_1 Q_1 \propto \{\frac{1}{C_\pi}, \frac{1}{C_\mu}\},$$

$$\frac{\omega_0 Q}{\omega_1 Q_1} \to \text{constant.}$$

Equation (17) can be denoted as equation (18), which indicates that in this case the total noise depends on the parasitic resistance and base current, transistor Q_{21} always contribute noise.

$$\int_0^\infty \frac{\overline{V_{outn}^2(f)}}{\Delta f} df \propto \{r_i, I_j\} \quad (i = e, b, \pi; j = B, C) \quad (18)$$

5 Numerical Examples

This section shows the effect of the parasitic resistance on the noise performance of the major noise contributor through numerical example.

In hold mode of SEF THA shown in Fig.5 of [1], for simplicity, we choose $r_\pi = r_e = r_b = r_0 = r$, $I_B = I_C = I$, $R_\mu = 0$. Equation (17) is denoted by equation (19), which indicates that the total noise of the output depends on both the thermal noise and shot noise. By choosing $q = 1$, $g_m = 100$ and knowing that $K_b T = 4.14 \times 10^{-21} J$, the equation (19) is further simplified as equation (20), this can be illustrated in Fig.5, which indicates both thermal noise and shot noise contributes to the total output noise. Therefore, in order to reduce the noise effect of SEF THA, decreasing the output noise of the major noise contributor Q_{21} is an effective solution. One approach is decreasing the magnitude of noise source o the transistor Q_{21} by adjusting the device geometric size.

$$\int_0^\infty \frac{\overline{V_{gn}^2(f)}}{\Delta f} df = \frac{2K_B Tr(16K_B Tr - 8\sqrt{2K_B Tqr I} + \frac{8q}{g_m})}{2K_B Tr + g_m q I} \quad (19)$$

$$\int_0^\infty \frac{\overline{V_{gn}^2(f)}}{\Delta f} df = \frac{5.48 \times 10^{-19} r^2 - 6.02 \times 10^{-9}\sqrt{rI} + 8 \times 10^{-2}}{8.28r + I \times 10^{23}} \quad (20)$$
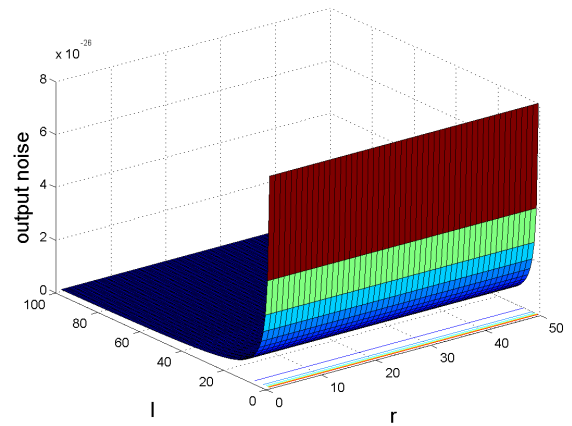

Figure 5: Output noise vs parasitic resistance(r) and base current(I)

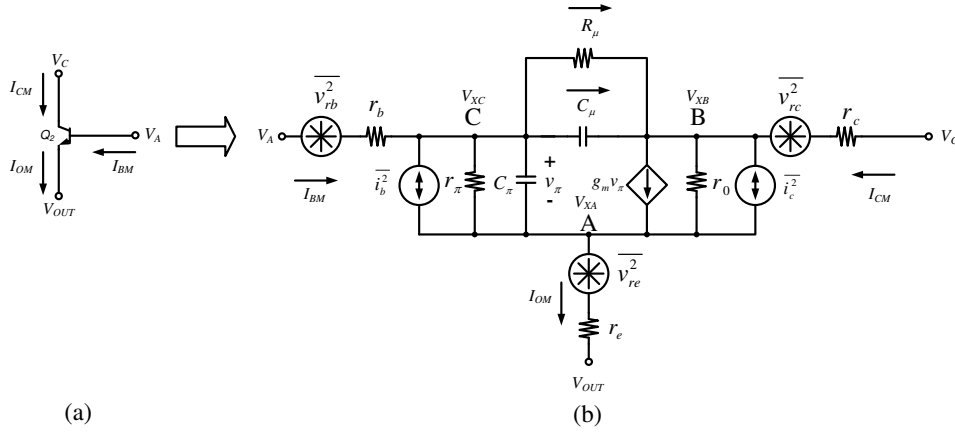(a)   (b)

Figure 4: Simplified small signal equivalent circuit of major noise contributor

$$V_{out} = \frac{1}{s^2 F + sG + H_4} [-s^2(K_1 V_{re} + L_1 V_{rb} + H_1) - s(K_2 V_{re} + L_2 V_{rb} + M_1 i_b + N_1 i_c + H_2)$$
$$- (K_3 V_{re} + L_3 V_{rb} + M_2 i_b + N_2 i_c + H_3)]$$

(14)

Where

$K_1 = r_0 C_\mu R_\mu C_\pi r_\pi,$

$K_2 = (r_0 C_\mu R_\mu g_m r_\pi + C_\pi r_\pi r_0 + C_\mu R_\mu r_\pi + R_\mu C_\pi r_\pi + r_0 C_\mu R_\mu),$

$K_3 = (g_m r_\pi r_0 + r_\pi + r_0 + R_\mu),$

$L_1 = r_0 C_\pi r_\pi C_\mu R_\mu,$

$L_2 = (C_\mu r_0 R_\mu + C_\pi r_\pi r_0 + R_\mu C_\pi r_\pi + r_\pi C_\mu R_\mu + r_0 g_m r_\pi C_\mu R_\mu),$

$L_3 = (g_m r_\pi r_0 + r_0 + R_\mu + r_\pi),$

$M_1 = -r_0 C_\mu R_\mu r_\pi,$

$M_2 = -(R_\mu r_\pi + r_\pi r_0),$

$N_1 = -r_0 R_\mu r_\pi C_\mu,$

$N_2 = -r_\pi r_0,$

$H1 = r_0 C_\mu R_\mu C_\pi r_\pi I_{OM} r_e + r_0 C_\pi r_\pi C_\mu R_\mu + r_0 C_\pi r_\pi C_\mu R_\mu I_{BM} r_b - r_0 C_\pi r_\pi C_\mu R_\mu V_a,$

$H2 = +r_0 C_\mu R_\mu I_{OM} r_\pi + C_\mu r_0 R_\mu I_{BM} r_b + C_\pi r_\pi r_0 I_{BM} r_b + R_\mu C_\pi r_\pi I_{OM} r_e + C_\mu R_\mu r_\pi I_{OM} r_e$
$\quad + r_0 C_\mu R_\mu I_{OM} r_e + r_0 C_\mu R_\mu g_m r_\pi I_{OM} r_e - C_\mu r_0 R_\mu V_a - C_\pi r_\pi r_0 V_a - R_\mu C_\pi r_\pi V_a - r_\pi C_\mu R_\mu V_a$
$\quad + R_\mu C_\pi r_\pi I_{BM} r_b + r_\pi C_\mu R_\mu I_{BM} r_b - r_0 g_m r_\pi C_\mu R_\mu V_a + r_0 g_m r_\pi C_\mu R_\mu I_{BM} r_b + C_\pi r_\pi r_0 I_{OM} r_e,$

$H3 = -R_\mu V_a + I_{BM} r_\pi R_\mu + g_m r_\pi r_0 I_{OM} r_e - g_m r_\pi r_0 V_a + I_{OM} r_\pi r_0 + r_0 I_{BM} r_b + R_\mu I_{BM} r_b$
$\quad + r_\pi I_{BM} r_b + g_m r_\pi r_0 I_{BM} r_b - r_0 V_a - r_\pi V_a + r_\pi I_{OM} r_e + r_0 I_{OM} r_e + R_\mu I_{OM} r_e,$

$H_4 = r_\pi + r_0 + g_m r_\pi r_0 + R_\mu,$

$F = r_0 C_\pi r_\pi C_\mu R_\mu,$

$G = C_\mu r_0 R_\mu + R_\mu C_\pi r_\pi + C_\pi r_\pi r_0 + r_\pi C_\mu R_\mu + r_0 g_m r_\pi C_\mu R_\mu.$

$$V_{out} = \frac{1}{s^2 F + sG + H_4} [-s^2(K_1 V_{re} + L_1 V_{rb}) - s(K_2 V_{re} + L_2 V_{rb} + M_1 i_b + N_1 i_c)$$
$$- (K_3 V_{re} + L_3 V_{rb} + M_2 i_b + N_2 i_c)]$$

$$= \frac{-(K_3 V_{re} + L_3 V_{rb} + M_2 i_b + N_2 i_c)}{H_4} \left(\frac{\frac{s^2}{\omega_1^2} + \frac{s}{\omega_1 Q_1} + 1}{\frac{s^2}{\omega_0^2} + \frac{s}{\omega_0 Q} + 1} \right)$$

(15)

Where

$$\omega_0 = \frac{H_4}{F}, \omega_0 Q = \frac{H_4}{G}, \omega_1 = \frac{K_3 V_{re} + L_3 V_{rb} + M_2 i_b + N_2 i_c}{K_1 V_{re} + L_1 V_{rb}}, \omega_1 Q_1 = \frac{K_3 V_{re} + L_3 V_{rb} + M_2 i_b + N_2 i_c}{K_2 V_{re} + L_2 V_{rb} + M_1 i_b + N_1 i_c}.$$

Where

$$\alpha = (K_3^2 r_e + L_3^2 r_b + 2K_3 L_3 \sqrt{r_e r_b}), \beta = (2K_3 M_2 \sqrt{r_e I_B} + 2K_3 N_2 \sqrt{r_e I_c} + 2L_3 M_2 \sqrt{r_b I_B} + 2L_3 N_2 \sqrt{r_b I_c}),$$
$$\gamma = (M_2^2 I_B + N_2^2 I_C + 2M_2 N_2 \sqrt{I_B I_C}).$$

$$\overline{\frac{V_{out}^2}{\Delta f}} = \left(\frac{-(K_3 V_{re} + L_3 V_{rb} + M_2 i_b + N_2 i_c)}{H_4}\right)^2 \frac{1}{\Delta f} \left|\frac{\frac{s^2}{\omega_1^2} + \frac{s}{\omega_1 Q_1} + 1}{\frac{s^2}{\omega_0^2} + \frac{s}{\omega_0 Q} + 1}\right|^2 = \frac{1}{H_4^2} \left|\frac{\frac{s^2}{\omega_1^2} + \frac{s}{\omega_1 Q_1} + 1}{\frac{s^2}{\omega_0^2} + \frac{s}{\omega_0 Q} + 1}\right|^2 [4K_B T\alpha + 2\sqrt{2K_B Tq}\beta + 2q\gamma] \quad (16)$$

$$\int_0^\infty \overline{\frac{V_{out}^2(f)}{\Delta f}} df = \frac{4K_B T\alpha + 2\sqrt{2K_B Tq}\beta + 2q\gamma}{H_4^2} \int_0^\infty \left|\frac{\frac{s^2}{\omega_1^2} + \frac{s}{\omega_1 Q_1} + 1}{\frac{s^2}{\omega_0^2} + \frac{s}{\omega_0 Q} + 1}\right|^2 df \approx \frac{4K_B T\alpha + 2\sqrt{2K_B Tq}\beta + 2q\gamma}{H_4^2} \frac{\omega_0 Q}{\omega_1 Q_1} \quad (17)$$

6 Simulation Results

Traditional circuit simulators such as HSPICE or SWIT-CAP have limitations in noise analysis by using a transistor-level description for the switched circuit. SpectreRF circuit simulator is capable of performing small signal analyses such as AC and noise about a periodic operating point and so can directly measure the transfer and noise characteristics of the switched circuit using a transistor-level description.

In our simulations, a commercial available 130 nm SiGe HBT process technology is used, the input source frequency is set as 16GHz, the clock source CLK_P is set as 40GHz, CLK_N is the complementary clock signal of CLK_P. The beat period is calculated from the reciprocal of the beat frequency from the fundamental tones. Running the Periodic Steady State analysis (PSS) and Periodic Noise analysis (PNoise) in SpectreRF simulator for the SEF THA shown in Fig.5 in [1] produces the total needed information for noise analysis. The noise figure in track mode and hold mode of the SEF THA is shown in Fig.6, which illustrates that hold mode contributes more noise to THA than track mode does. Thus it is important to investigate the noise behavior in hold mode to improve the dynamic noise performance.
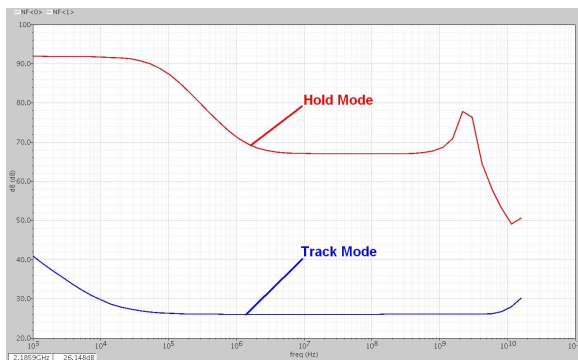

Figure 6: The noise figure in track mode and hold mode of SEF THA

It is valuable to know the main contributors of noise in the hold mode of SEF THA, Fig.7 illustrates the top 5 noise contributed instances from THA.

It can be seen from the noise summary in Fig.7 that except the introduced testing port4 the instance Q_{21} (Q_2 of Fig.5 in [1]) contributes more output noise than other instances. This can also be shown from the seperate instance noise in Fig.8.
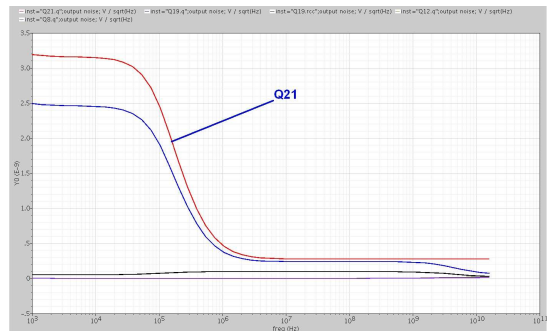

Figure 7: Noise summary

Figure 8: Noise contribution from the instances

The total output noise of the SEF THA is illustrated in Fig.9, the variation trend is similar to the numerical analysis results shown in Fig.5.

It is obvious that Q_{21} is the major noise contributor in the hold mode of THA. To improve the noise performance of the THA, reducing the output noise of Q_{21} is an effective solution. An effective approach to decrease the magnitude of noise source Q_{21} is adjusting the geometric size of this transistor. This can be justified by doing the noise simulation with only reducing the width of Q_{21} and its corresponding differential device to be a half . Figure.10 shows the noise contributed by the instance Q_{21} with the half size of the width. Compare with Figure.8, it shows that the magnitude of noise source Q_{21} becomes smaller as its size decreases. Figure.11 illustrates the total out-
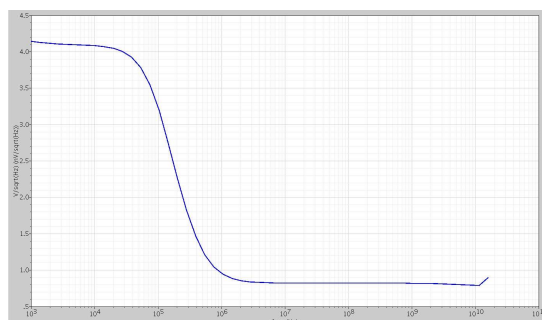
Figure 9: Total output noise of the SEF THA

put noise for the case simulating with the smaller size of Q_{21}. Compare with Figure.9, it demonstrates that the the total output noise drops down when the geometric size of the major noise contributor reduces.
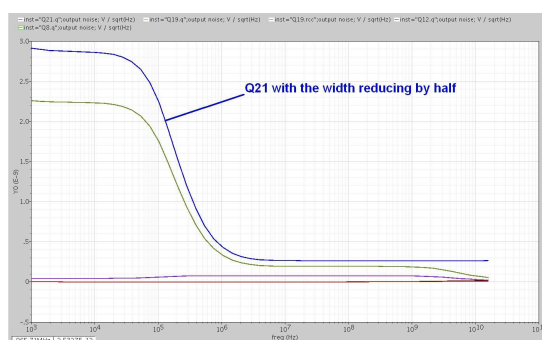

Figure 10: Noise contribution from the instances with the width of Q_{21} reducing by half
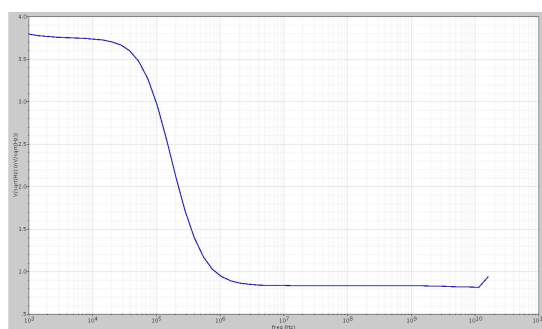

Figure 11: Total output noise of the SEF THA with the width of Q_{21} reducing by half

7 Conclusions

The noise analysis for the SEF configuration THA is presented. Simulation based on SpectreRF locates the major noise contributor to THA. Approximate expression of the output noise is given and shows that the dominant noise is thermal noise and shot noise. Theoretical noise analysis and numerical analysis for the major noise contributor of SEF THA show that at ultra high frequency the noise contribution by both thermal noise and shot noise is significant.

Acknowledgments

References

[1] S. Shahramian, A. C. Carusone, and S. P. Voinigescu, "Design methodology for a 40-GSamples/s track and hold amplifier in 0.18-μm SiGe BiCMOS technology," *IEEE Journal of Solid-State Circuits*, vol. 41, no. 10, pp. 2233 – 2240, sep.2006.

[2] Y. Gai, R. Geiger, and D. Chen, "Noise analysis in hold phase for switched-capacitor circuits," *2008 51st IEEE International Midwest Symposium on Circuits and Systems (MWSCAS)*, pp. 45 – 8, 2008/08/10.

[3] P. Vorenkamp and J. P. Verdaasdonk, "Fully bipolar, 120-Msample/s 10-b track-and-hold circuit," *IEEE Journal of Solid-State Circuits*, vol. 27, no. 7, pp. 988 – 992, 1992.

[4] P. R. Gray and R. G. Meyer, *Analysis and Design of Analog CMOS Integrated Circuits.* JOHN WlLEY & SONS, INC ,Newyork, 2001.

[5] M. Rudolph, R. Doerner, L. Klapproth, and P. Heymann, "An HBT noise model valid up to transit frequency," *IEEE Electron Device Letters*, vol. 20, no. 1, pp. 24 – 6, 1999.

[6] K. Yau, "Noise Modelling of Silicon-Germanium Heterojunction Junction Bipolar Transistors At Millimeter-Wave Frequencies," Master's thesis, University of Toronto, 2006.